Air Force Avionics Laboratory
Research and Technology Division
Air Force Systems Command
Wright-Patterson Air Force Base, Ohio

TRANSMITTER IMPEDANCE CHARACTERISTICS FOR AIRBORNE SPECTRUM SIGNATURE

Interim Technical Report No. 1
1 April - 30 June 1966

J. E. Ferris, W. DeHart, R. L. Wolford and W. B. Henry

15 July 1966

Contract AF-33(615)-3454

Contract Monitor: K. W. Tomlinson AVWE

7956-1-T = RL-2166

THE UNIVERSITY OF MICHIGAN
COLLEGE OF ENGINEERING
DEPARTMENT OF ELECTRICAL ENGINEERING
Radiation Laboratory

Administered through:
OFFICE OF RESEARCH ADMINISTRATION · ANN ARBOR

TABLE OF CONTENTS

ABSTRACT

Under a previous contract, AF-33(615)-2606, an investigation was made of measurement techniques applicable to the accurate determination of spectrum signatures of airborne transmitters. It was shown that in principle, only three measurements are required for the prediction of power radiated from a transmitter-antenna combination. These are: (1) the antenna VSWR, (2) the transmitter VSWR, and (3), the maximum power available from the transmitter. In this report, a method is described for obtaining the antenna VSWR under circumstances that would otherwise result in interference to other systems. A small anechoic chamber used to isolate the antenna is described and the chamber's performance is evaluated.

When determining the impedance (or VSWR) of a transmitter at the fundamental, spurious and harmonic frequencies, it is necessary to employ a frequency selective detector. The modification of an APR-4 radar receiver for incorporation in a frequency selective detection system is described in this report. The techniques for measuring the impedance of a transmitter, developed under the above contract, are based on the assumption of transmitter linearity. This report describes an investigation of the linearity of sample transmitters. Determination of source linearity is best accomplished through the use of the Rieke diagram. Rieke diagrams, at the fundamental frequency, for three types of sources are presented and the results are discussed. Also included is a discussion of source non-linearity at harmonic and spurious frequencies.

I. INTRODUCTION

The statement of problem as set forth in the contract which provides for the present investigation is as follows.

A determination of the power delivered to the antenna for "spectrum signature" purposes will require a measurement of the antenna impedance, transmission line characteristics, transmitter maximum power output, and transmitter output impedance at the fundamental, spurious and harmonic frequencies. The transmitter output impedance at the spurious and harmonic frequencies is not well understood and, therefore, requires further study. The prime payoff in this study will be better "spectrum signatures" for more accurate predictions of interference between systems.

There is a need to verify the results of the earlier successful program, Contract AF 33(615)2606 "Simplified Modeling Techniques for Avionic Antenna Pattern Signatures", with a mock-up of an aircraft transmitter system.

The stated objective of the contract is: To conclude the development of "simplified" techniques for determining the RF spectrum signatures of flight vehicle electronics systems. To establish the validity of the techniques by comparing the results of data obtained by the "simplified" techniques with data obtained from tests employing a typical transmitter system in a mock-up.

A previous report (Ferris et al, 1966) discussed the theoretical aspects of power transfer under unmatched conditions: a subject of great importance in the prediction of spurious radiation from a transmitter - antenna combination. It was shown how, in principle, the power radiated can be predicted from measurements of the transmitter, transmission line, and antenna. Although two of these measurements (i.e., transmitter and antenna) involve simply the determination of standing wave ratios, the present study is being conducted under more stringent requirements, i.e., the determination of transmitter and antenna impedances. It is felt that this approach provides a more sound foundation for the verification of the simplified measurement techniques being developed.

II. COMPLEX LOAD IMPEDANCE MEASUREMENTS

In the final report (Ferris et al, 1966) on the predecessor contract, it was recommended that the technique developed by Michigan for measuring the impedance of a source be further evaluated by employing typical transmitters used by the military services. The source impedance measurement technique discussed in the above report utilizes as the terminating impedance either a short-circuit or a complex load. The use of either of these terminations has been experimentally verified by measurements of the impedance of a laboratory type signal generator and a tuning stub. When measuring the impedance of a typical transmitter used by the service, it may be impractical to use a short-circuit termination since the transmitter may be designed to work into a well matched load at the fundamental frequency. Thus, it will be necessary to use a complex load when making the impedance measurement and it appears logical to use the typical system antenna as the complex load to best satisfy all conditions. It has been shown that the only requirement pertaining to the use of the complex load is that it's VSWR be accurately known at the frequency of interest. The VSWR of the antenna must be known also for power transfer considerations. Further, the system antenna is the most convenient device to use in the field when making system measurements.

2.1 300 MHz Anechoic Chamber

In view of the above considerations to use the system antenna as the complex load when making source impedance measurements on a typical transmitter, a

300 MHz anechoic chamber was constructed. This enclosure will house the antenna for measurement purposes. The chamber will provide a free-space environment for the antenna since it is not always practical to make laboratory type investigations in the field. Stray reflections are undesirable when the VSWR of the antenna is being determined or the impedance (or VSWR) of the transmitter is being measured. If a relatively low power source is not available for determining the VSWR of the antenna, the chamber will allow the measurement to be made with the typical service transmitter which produces relatively high power (10 to 30 watts). In the event the transmitter is of the communications type as is being used in this investigation, the antenna must be electrically isolated from the surroundings so as not to cause interference to other systems in the locality. The 300 MHz chamber constructed by Michigan meets these requirements as will be shown below.

2.1.1 300 MHz Chamber Construction

The chamber consists of a 64 cubic foot cube as shown in Figure 2-1. Aluminum sheets are supported on the outside by a wood frame. All interior joints have been sealed to prevent rf leakage. The inside of the cube is lined on all six sides will broadband absorbing material covered with vinyl. An eight cubic foot volume of space is left in the interior of the chamber for the antenna installation. The absorber is described by the manufacturer as having moderate performance for frequencies of 300 MHz and up. Our evaluation has

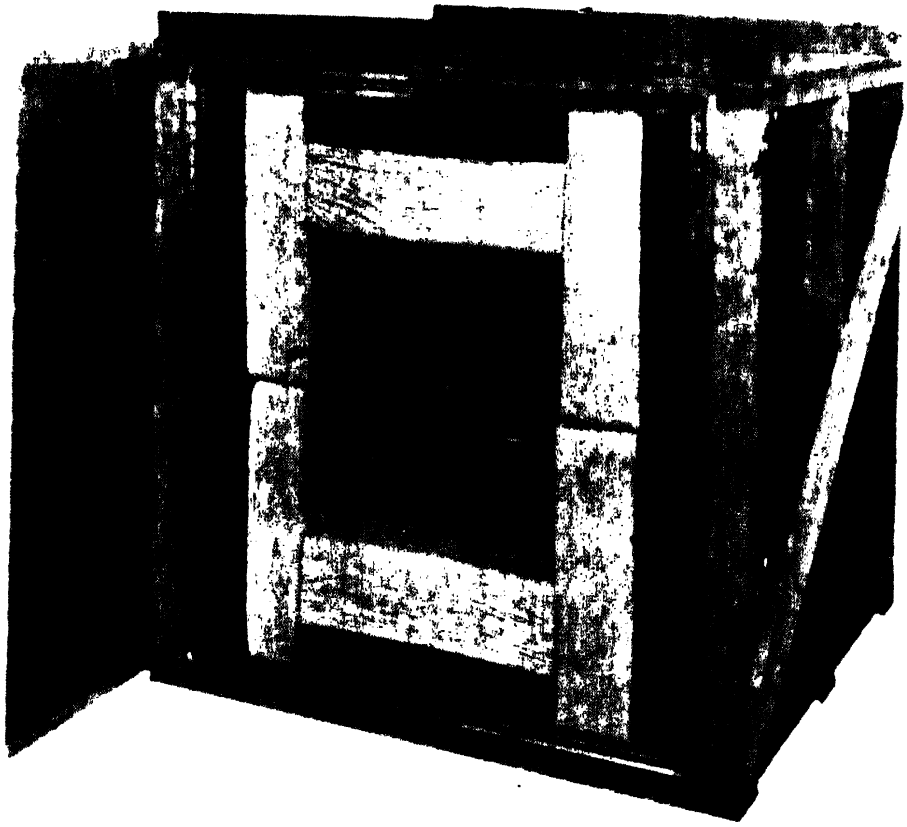

FIG. 2-1: 300 MHz ANECHOIC CHAMBER (With Blade antenna AT-256A/ARC-27)

shown the absorber to perform effectively at 200 MHz and higher. Electronic gasketing has been installed to prevent rf leakage around the door which forms one side of the chamber.

2.1.2 300 MHz Chamber Evaluation

The chamber was tested for its effectiveness as a free-space environment by comparing impedance data taken for two typical military antennas, inside and outside the chamber. The two antennas measured were the blade antenna AT-256A/ARC-27, and the modified monopole antenna, both of which are designed to operate over the frequency range of 200 - 400 MHz. An impedance plot for the blade antenna from 200 - 1500 MHz is shown in Fig. 2-2. The impedance data for the antenna inside the chamber, shown in Fig. 2-1, is superimposed on the data taken in a free-space environment in the field, shown in Fig. 2-3. As can be seen from Fig. 2-2, the two sets of data compare favorably. Agreement is typically within 10 percent. Measurement inaccuracies are felt to be responsible for the few data points not demonstrating the typical agreement. Data for the modified monopole is not shown due to a delay in data reduction.

No. GC 1950⁹

NAME	TITLE	DWG. NO.
SMITH CHART FORM 530-7560-N	GENERAL RADIO COMPANY, WEST CONCORD, MASSACHUSETTS	DATE

IMPEDANCE OR ADMITTANCE COORDINATES

⊙ Outdoor Environment

△ Chamber Environment

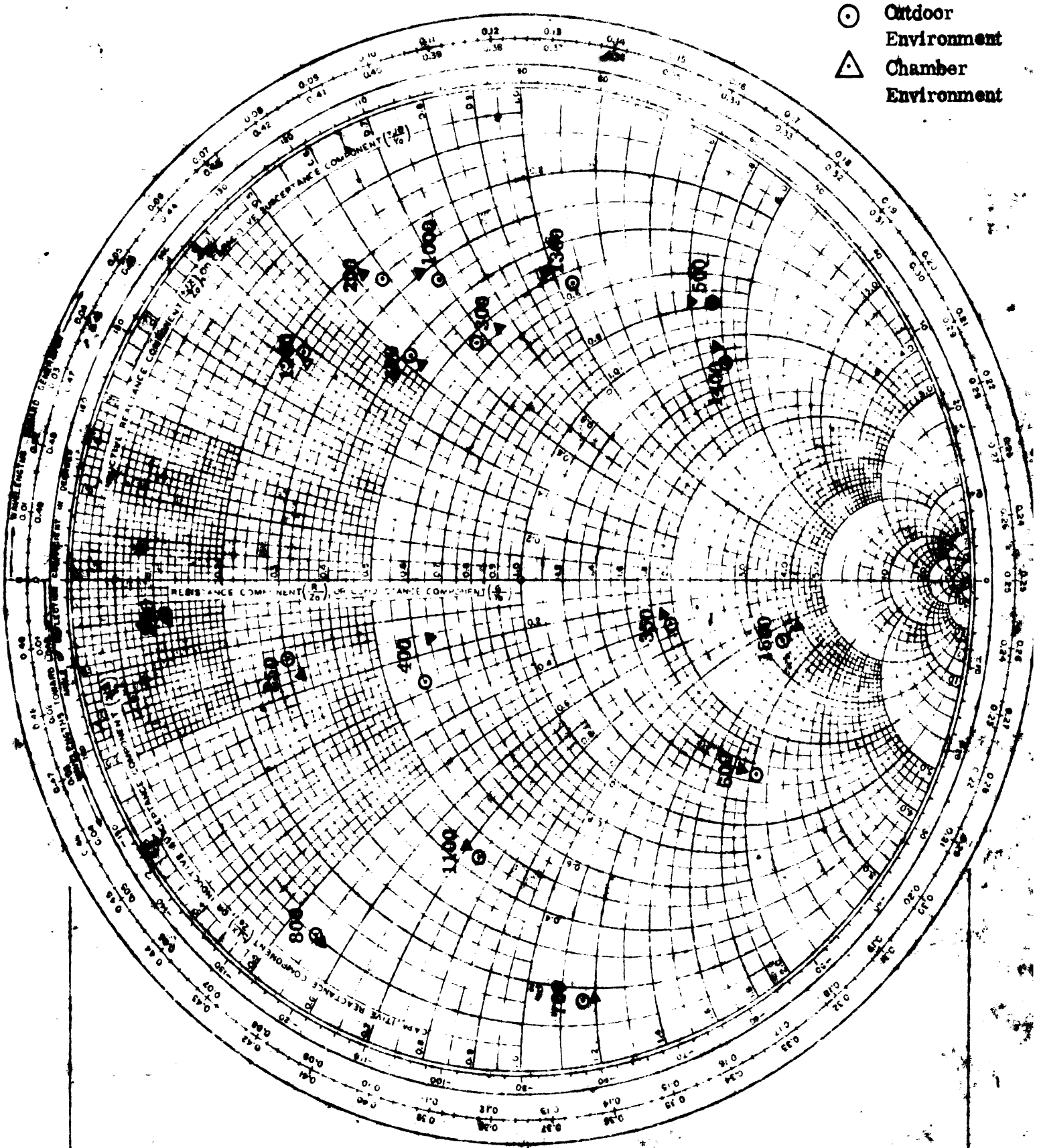

FIG. 2-2: IMPEDANCE CHARACTERISTICS OF BLADE ANTENNA AT-256A/ARC-27

RADIALLY SCALED PARAMETERS (Frequency in MHz)

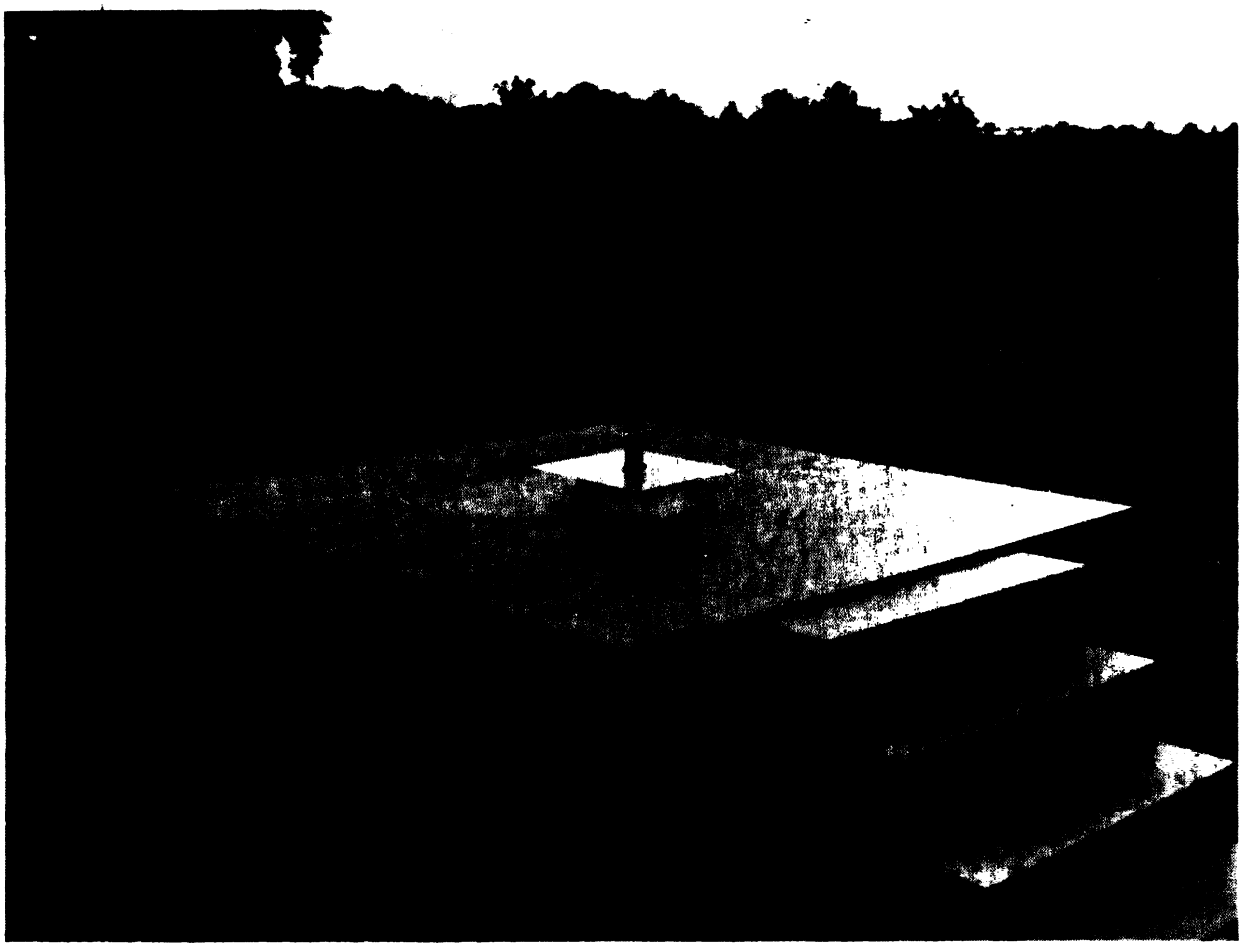

FIG. 2-3: BLADE ANTENNA AT-256A/ARC-27 ON OUTDOOR IMPEDANCE PLATFORM

III. SOURCE IMPEDANCE MEASUREMENTS

Techniques for measuring the impedance of a source have been developed and were presented in the final report (Ferris et al, 1966) on the predecessor contract. The application of the techniques to date has been very successful. The accuracies attained are sufficient for the prediction of power transfer to the antenna at the fundamental frequency. The above report contains the results of laboratory measurements of source impedance of a signal generator. The present study involves the application of these measurement techniques to a typical service transmitter at the fundamental, spurious and harmonic frequencies. This type of source presents the investigator with complications not previously encountered with the laboratory type signal generator. Therefore, before applying the measurement techniques to the transmitter, consideration has been given to the need for a frequency selective detection system, and an investigation of the nonlinear characteristics of the source.

3.1 Need For A Frequency Selective Receiver

In order to determine the impedance of a transmitter at the fundamental, spurious and harmonic frequencies, one must be able to detect and measure only the frequency of interest. The impedance measurement technique requires measurement of the standing wave produced on the line at the frequency of interest. Since the typical transmitter produces several spurious and harmonic frequencies in addition to the fundamental, several standing waves appear on the line simultaneously.

The apparatus used to detect the desired frequency must then obviously be frequency selective. Therefore, consideration has been given to the modification of an APR-4 radar receiver to be incorporated in a frequency selective detection system for the source impedance measurements.

3.1.1 Modification of the APR-4 Radar Receiver

An APR-4 radar receiver IF chassis and appropriate tuning heads have been obtained. The receiver is shown in Fig. 3-1. After checking and replacing defective components, the receiver IF was realigned with a sweep generator and oscilloscope until the response curve in the wide mode was similar to that in Fig. 3-2. Next, the circuit was modified as shown in Fig. 3-3, (the 6H6 detector was removed) and the IF output was connected to a type N connector, which was installed in place of the VHF "Pan" output connector. Finally, the appropriate receiver tuning units were tuned and installed.

Following the above preparations, the sensitivity and linearity of the unit were measured. The sensitivity of the unit is approximately -65 dbm (minimum discernable signal). However, it should be noted that the sensitivity varies considerably with frequency. The receiver is linear (square law) within $\pm$ 1 db over a 35 - 40 db dynamic range. The performance of the unit is felt to be satisfactory for use in the frequency selective detection system.

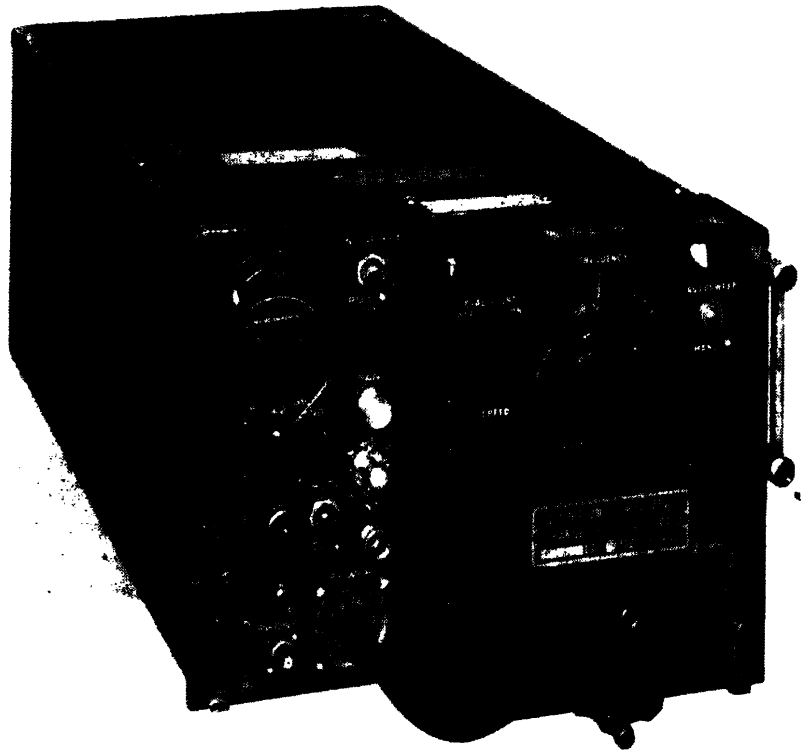

FIG. 3-1: APR-4 RADAR RECEIVER

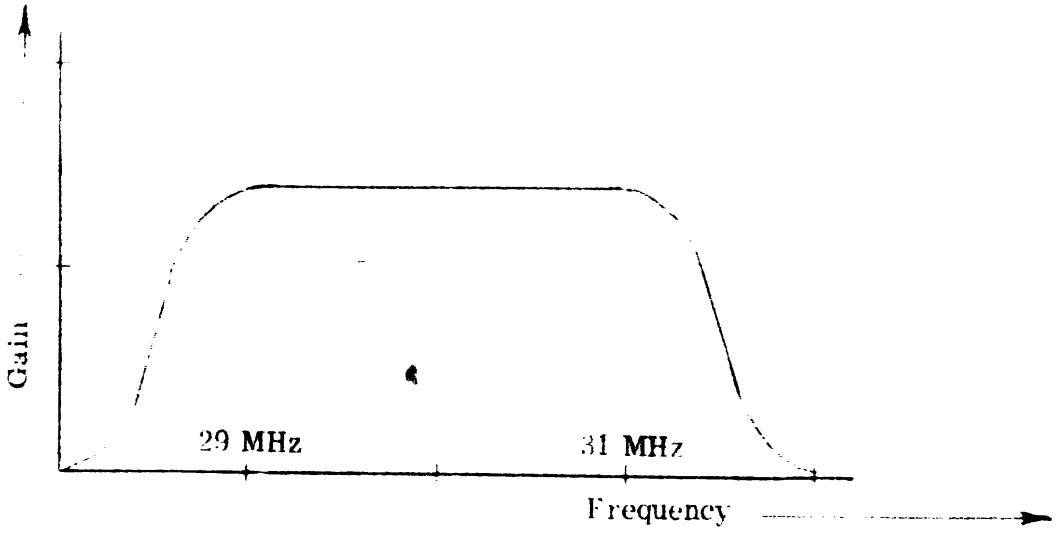

FIG. 3-2: IF RESPONSE CURVE

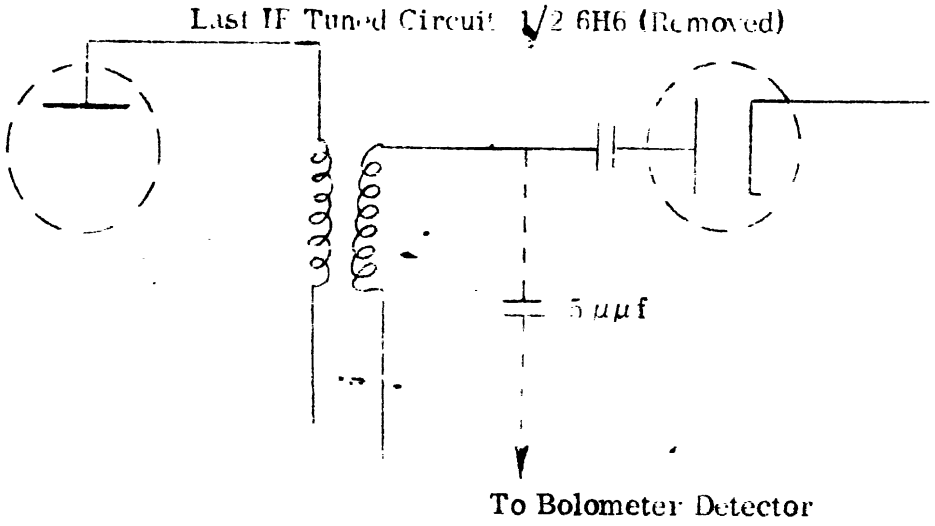

FIG. 3-3: APR-4 CIRCUIT MODIFICATION

3.2 Source Non-Linearity at the Fundamental Frequency

Expressions for power transfer on a transmission line are usually derived from a model similar to Fig. 3-4. It is usually thought reasonable to assume that the generator impedance Z_g is not a function of the load impedance, e.g., the model is a linear model. This assumption may or may not be accurate depending upon the particular generator used and the variations in load impedance. A convenient method by which the accuracy of the assumption may be determined for a particular generator is to compare Rieke diagrams of the linear model and the real generator. A Rieke diagram is a plot on the complex impedance (Smith) chart of constant power contours. A constant power contour for a constant source impedance can be shown to be a circle. A comparison of the actual constant power contour obtained by experiment and the theoretical contour of a linear model shows the variation of the source impedance as a function of the load impedance.

3.2.1 Theoretical Rieke Diagrams

Figure 3-4 is the model from which the diagrams will be plotted. The average steady-state power delivered to the load is the real part of the rms voltage appearing across the load multiplied by the complex conjugate of the rms current through the load.

$$P_l = \mathrm{Re}\left[E_l\, I_l^*\right] \tag{3.1}$$

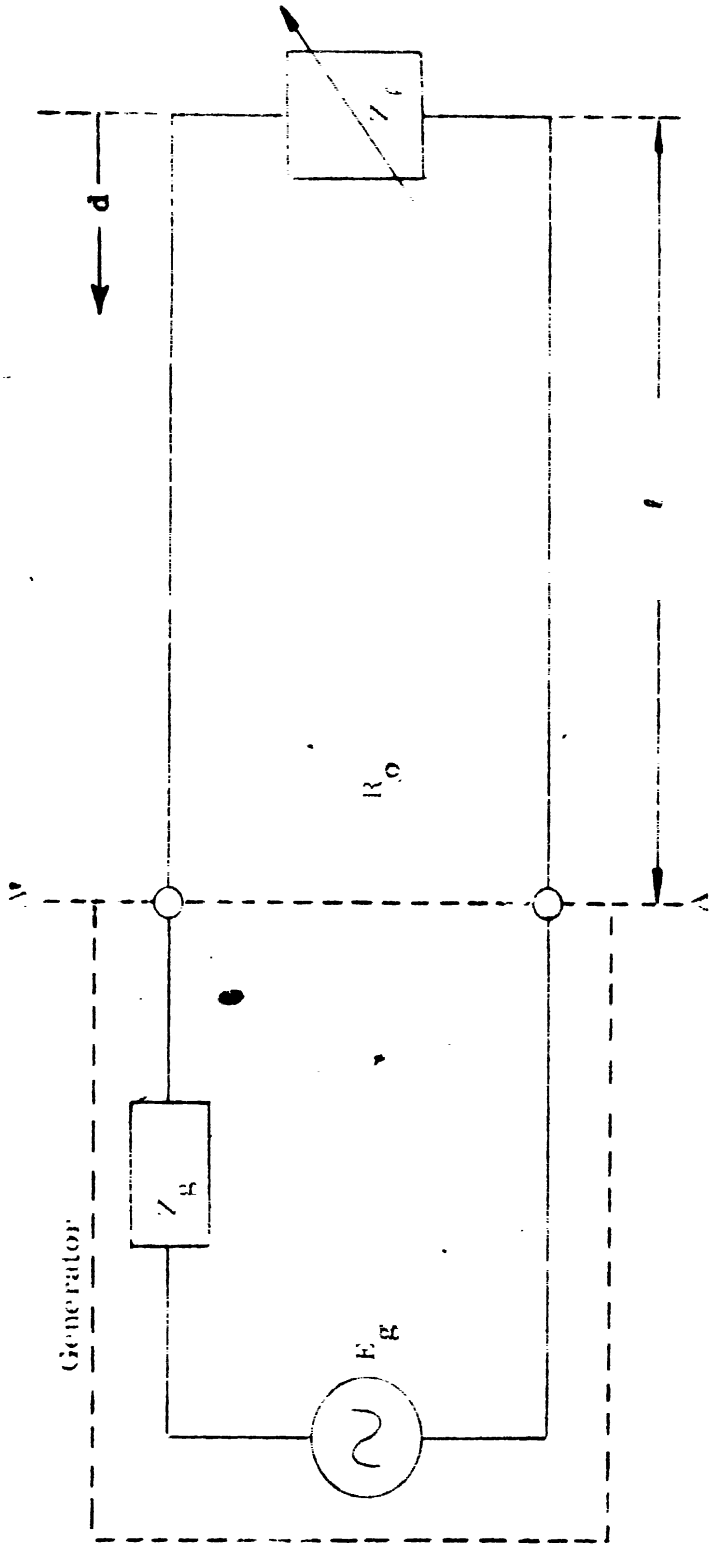

FIG. 3-4: SIMPLE POWER TRANSFER MODEL.

However, the load will not in general be located directly at the generator terminals. Let the impedance seen by looking into the line in the direction of the load at the plane A A' be Z_a. The average power delivered to Z_a is

$$P_a = \mathrm{Re}\left[E_a I_a^*\right] \tag{3.2}$$

where

$$I_a = \frac{E_g}{Z_g + Z_a} \quad \text{and} \quad E_a = I_a Z_a \tag{3.3}$$

thus

$$E_a = \frac{E_g}{Z_g + Z_a} Z_a \tag{3.4}$$

It is now evident that

$$P_a = \mathrm{Re}\left[\frac{E_g}{Z_g + Z_a} Z_a \cdot \left(\frac{E_g}{Z_g + Z_a}\right)^*\right] \text{ or} \tag{3.5}$$

$$P_a = \left|\frac{E_g}{Z_g + Z_a}\right|^2 \cdot R_a = \frac{|E_g|^2 R_a}{(R_g + R_a)^2 + (X_g + X_a)^2} \; + \tag{3.6a,b}$$

The result (3.6b) may be reduced to a more convenient form. Since it is of interest to plot constant power contours as a function of Z_a, define a constant K_n such that

$$K_n = \frac{|E_g|^2}{P_{a_n}} \tag{3.7}$$

+ Where the complex impedance Z_a has been expressed as $Z_a = (R_a + jX_a)$

Combining (3.6, b) and (3.7),

$$K_n R_a = R_a^2 + 2R_a R_a + R_g^2 + X_a^2 + 2X_n X_g + X_g^2 \qquad (3.8)$$

Rearranging (3.8) and completing the square yields

$$\left[R_a + \frac{2R_g - K_n}{2}\right]^2 + \left[X_a + X_g\right]^2 = \frac{K_n^2 - 4K_n R_g}{4} \qquad (3.9)$$

Equation (3.9) is of the form $U^2 + V^2 = A^2$, implying that Rieke diagrams plotted on a rectangular chart (R_a, abscissa; jX_a, ordinate) and assuming a constant generator internal impedance, will be circles with center at

$\left(\frac{K_n}{2} - R_g\right), \left(-X_g\right)$ and radius $\left[\frac{K_n^2 - 4K_n R_g}{4}\right]^{1/2}$. Furthermore, for the radius to be real

$$K_n^2 \geq 4K_n R_g \qquad (3.10)$$

which implies that

$$P_a \leq \frac{|E_g|^2}{4R_g}, \qquad (3.11)$$

i.e., the maximum power available to the load can never exceed the square of the generator voltage divided by four times the real part of the generator impedance.

The load impedance corresponding to maximum generator power output for a given lead impedance can be found directly from

$$P_a = \frac{|E_g|^2 R_a}{(R_g + R_a)^2 + (X_g + X_a)^2} \qquad (3.6b)$$

Obviously P_a will be a maximum when $\left(X_g + X_a\right)$ is a minimum, specifying that $X_a = -X_g$. $P_{a\,(max)}(R_a)$ is determined by setting

$$\frac{dP_a}{dR_a} = 0.$$

$$\frac{dP_a}{dR_a} = \frac{\left(R_g + R_a\right)^2 |E_g|^2 - E_g^2 R_a \left(2R_a + 2R_g\right)}{\left(R_g + R_a\right)^4} = 0 \tag{3.12}$$

$$0 = R_g^2 + 2R_g R_a + R_a^2 - 2R_a^2 - 2R_g R_a = R_g^2 - R_a^2 \tag{3.13}$$

Since the values of R_a and R_g are restricted to positive real numbers, (3.13) reduces to

$$R_g = R_a \tag{3.14}$$

Thus we have the familiar result that maximum power transfer results when the load impedance at the generator terminals is the complex conjugate of the generator impedance. Substituting this result into (3.6b)

$$P_{a(max)} = \frac{|E_g|^2}{4R_g} \tag{3.15}$$

verifying (3.11).

The result (3.9) may also be expressed in terms of the load impedance Z_l and length of lossless transmission line by substituting an expression for Z_a in terms of Z_l.

$$Z_a = R_o \left[\frac{Z_\ell \cos \beta\ell + jZ_o \sin \beta\ell}{Z_o \cos \beta\ell + jZ_\ell \sin \beta\ell} \right] \tag{3.16}$$

where $\beta = \frac{2\pi}{\lambda}$, and ℓ is the electrical transmission line length from the generator terminals to the load.

Equation (3.9) lends itself readily to mapping on a rectangular impedance chart or it may be point plotted on a Smith Chart. One method for mapping (3.9) on a Smith Chart is to recognize that circles on a rectangular chart transform to circles on the Smith Chart. It is now necessary only to plot three points from (3.9) on the Smith Chart and draw a circle whose circumference includes the points. The center of the circle is located by the intersection of the perpendicular bisectors of straight lines joining the points.

A less tedious method involves a transformation of variables from the Z plane to the ρ plane. It has been shown that a bilinear transformation of a circle in one complex plane yields a circle in the second (Guillemin, 1949). Thus the circle defined in the Z-plane by equation (3.9) transforms to a circle in the ρ plane, the transformation equation being

$$Z = \frac{1 + \rho}{1 - \rho} \tag{3.17}$$

Reich, Ordung, Krauss, and Skolnik (1953) have demonstrated that the circle

$$Z = r_o + jx_o + Re^{j\alpha} \tag{3.18}$$

with center at (r_o, jx_o) and radius R in the Z-plane transforms to the circle,

$$Z = \left|\rho_o\right| e^{j\beta_o} + R_\rho e^{j\alpha_\rho} \tag{3.19}$$

in the ρ plane. In terms of the parameters of (3.18)

$$R_\rho = \frac{2R}{\left(r_o + 1\right)^2 + x_o^2 - R^2} \tag{3.20}$$

$$\left|\rho_o\right| = \left\{\left[\frac{\left(r_o - 1\right)^2 + x_o^2 - R^2}{\left(r_o + 1\right)^2 + x_o^2 - R^2}\right]^2 + \left[\frac{-2x_o}{\left(r_o + 1\right)^2 + x_o^2 - R^2}\right]^2\right\}^{1/2} \tag{3.21}$$

$$\beta_o = \tan^{-1}\left(\frac{-2x_o}{r_o^2 - 1 + x_o^2 - R^2}\right) \tag{3.22}$$

Substituting

$$r_o = \frac{K_n - 2R_g}{2}, \quad x_o = -X_g, \text{ and } R = \left[\frac{K_n^2 - 4K_n R_g}{4}\right]^{1/2} \tag{3.23}$$

from (3.19) into (3.16), (3.17), and (3.18)

$$R_\rho = \frac{\left[K_n^2 - 4K_n R_g\right]^{1/2}}{\left(R_g - 1\right)^2 + K_n + X_g^2} \tag{3.24}$$

$$|\rho_o| = \frac{\left[\left(R_g^2 + X_g^2 - 1\right)^2 + 4X_g^2\right]^{1/2}}{\left(R_g - 1\right)^2 + K_n + X_g^2} \qquad (3.25)$$

$$\beta_o = \tan^{-1}\left[\frac{-2X_g}{\left|R_g^2 + X_g^2 - 1\right|}\right] \qquad (3.26)$$

Once the parameters of (3.9) have been determined, (3.9) can be mapped directly onto a Smith Chart as the circle (3.19) with center at $\left(|\rho_o|, \beta_o\right)$ and radius R_ρ.

Figures 3-5, 3-6, 3-7, and 3-8 are plots of (3.9) on rectangular and Smith charts. Figures 3-5 and 3-6 are the special case $R_g = R_o$, the transmission line impedance. In Figs. 3-7 and 3-8, $Z_g = 1.5 - j0.5$ (normalized). Notice that the loci of the centers of the circles form a straight line on each chart corresponding to a constant reactance on the rectangular chart and a constant angle of reflection coefficient on the Smith chart.

3.2.2 Experimental Rieke Diagrams

To investigate the internal impedance variations of a real generator, one must plot an experimental Rieke diagram of the generator. A convenient approach to the equipment setup is shown in Fig. 3-9. This is basically the arrangement which was used to collect the experimental data presented in this report. However, the presence of strong harmonic and spurious outputs would necessitate a more elaborate setup.

Figures 3-10 through 3-13 are experimental Rieke diagrams obtained with the equipment shown in Fig. 3-9. The figures include the ideal model contours superimposed on the experimental data points.

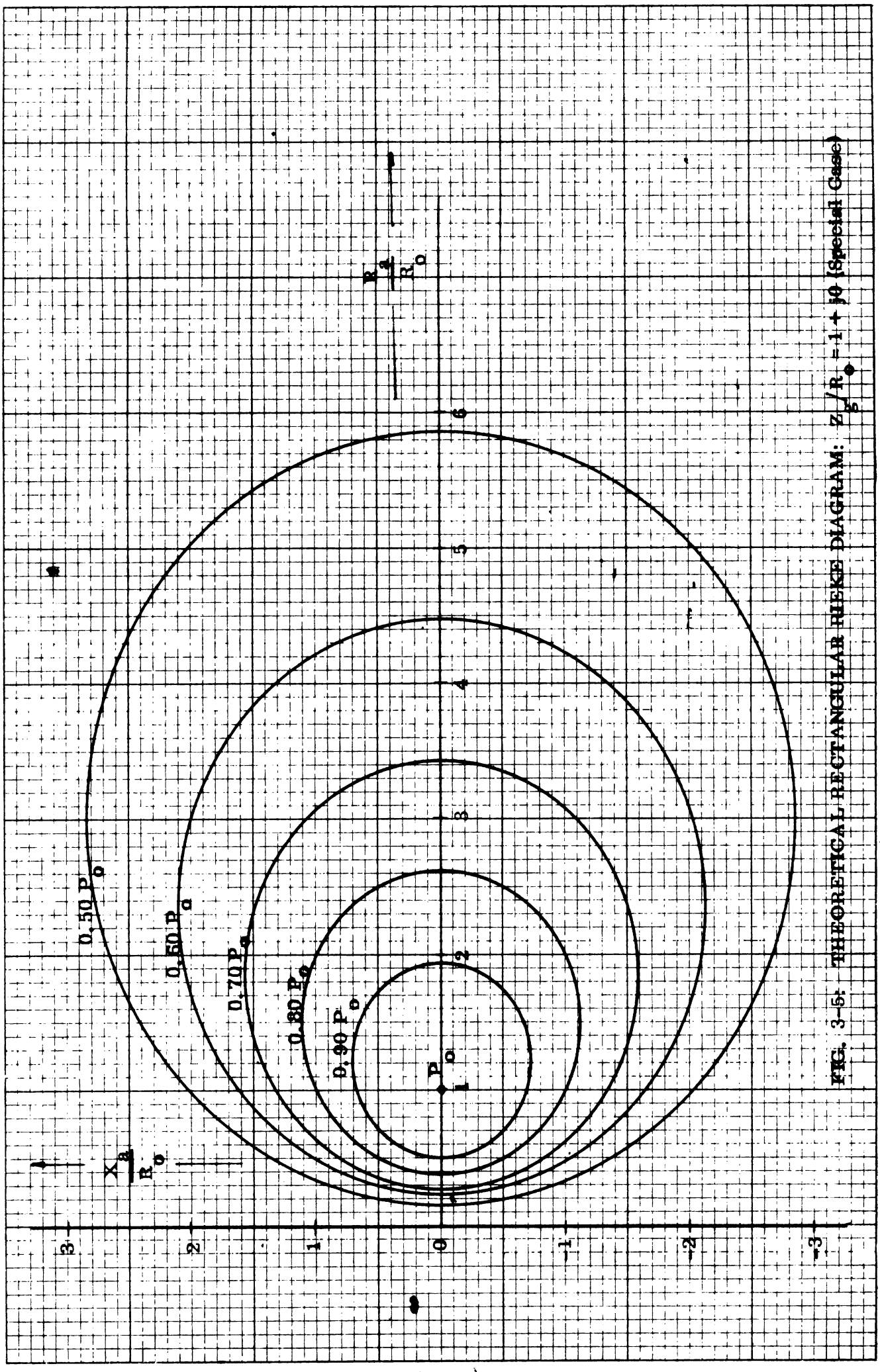

FIG. 3-6: THEORETICAL RECTANGULAR RIEKE DIAGRAM: $Z_s/R_o = 1 + j0$ (Special Case)

NAME	TITLE	DWG. NO.
SMITH CHART FORM 5301-7560-N	GENERAL RADIO COMPANY, WEST CONCORD, MASSACHUSETTS	DATE

IMPEDANCE OR ADMITTANCE COORDINATES

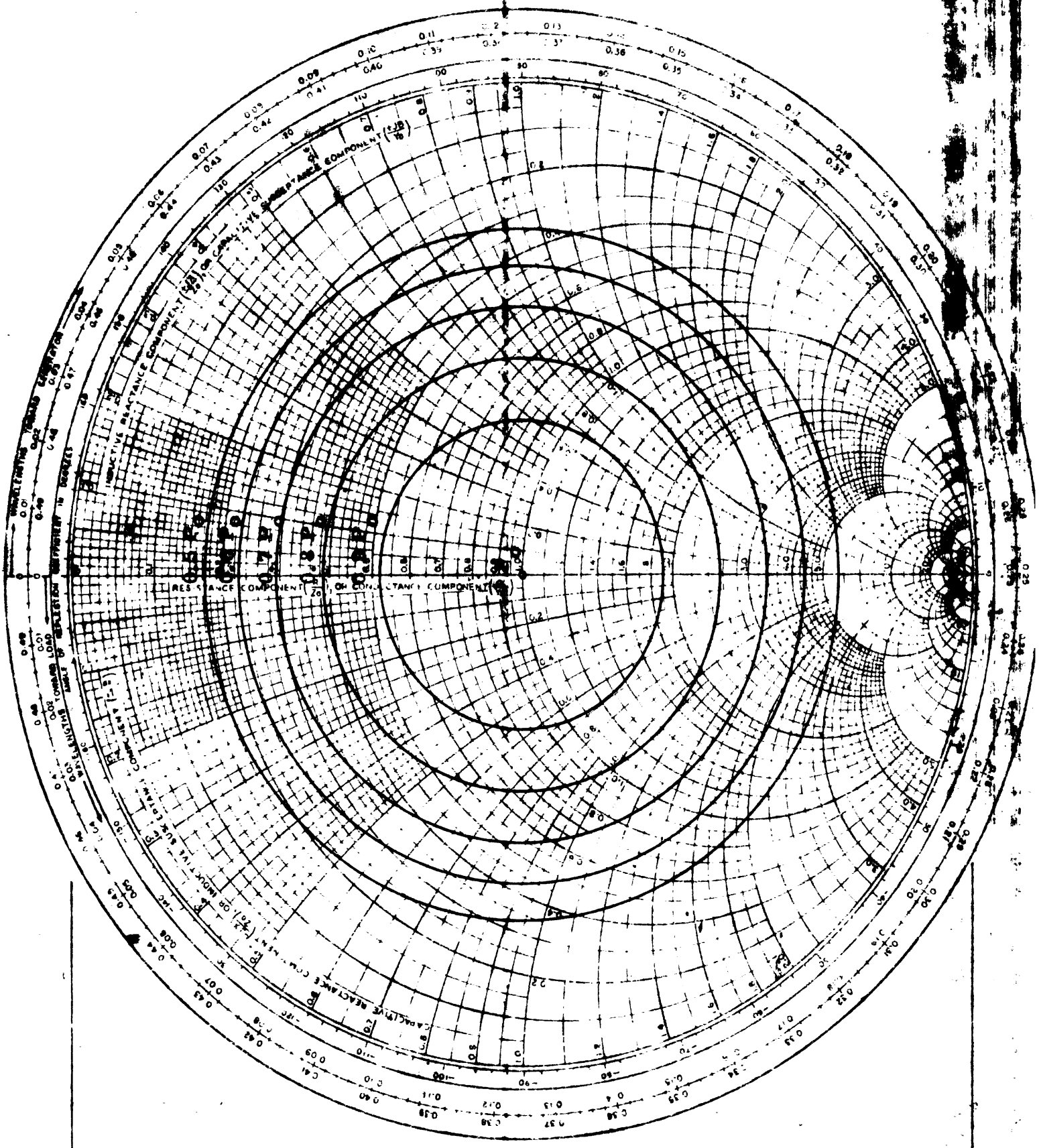

FIG. 3-6: THEORETICAL RIEKE DIAGRAM: $Z/R = 1 + j0$ (Special Case)

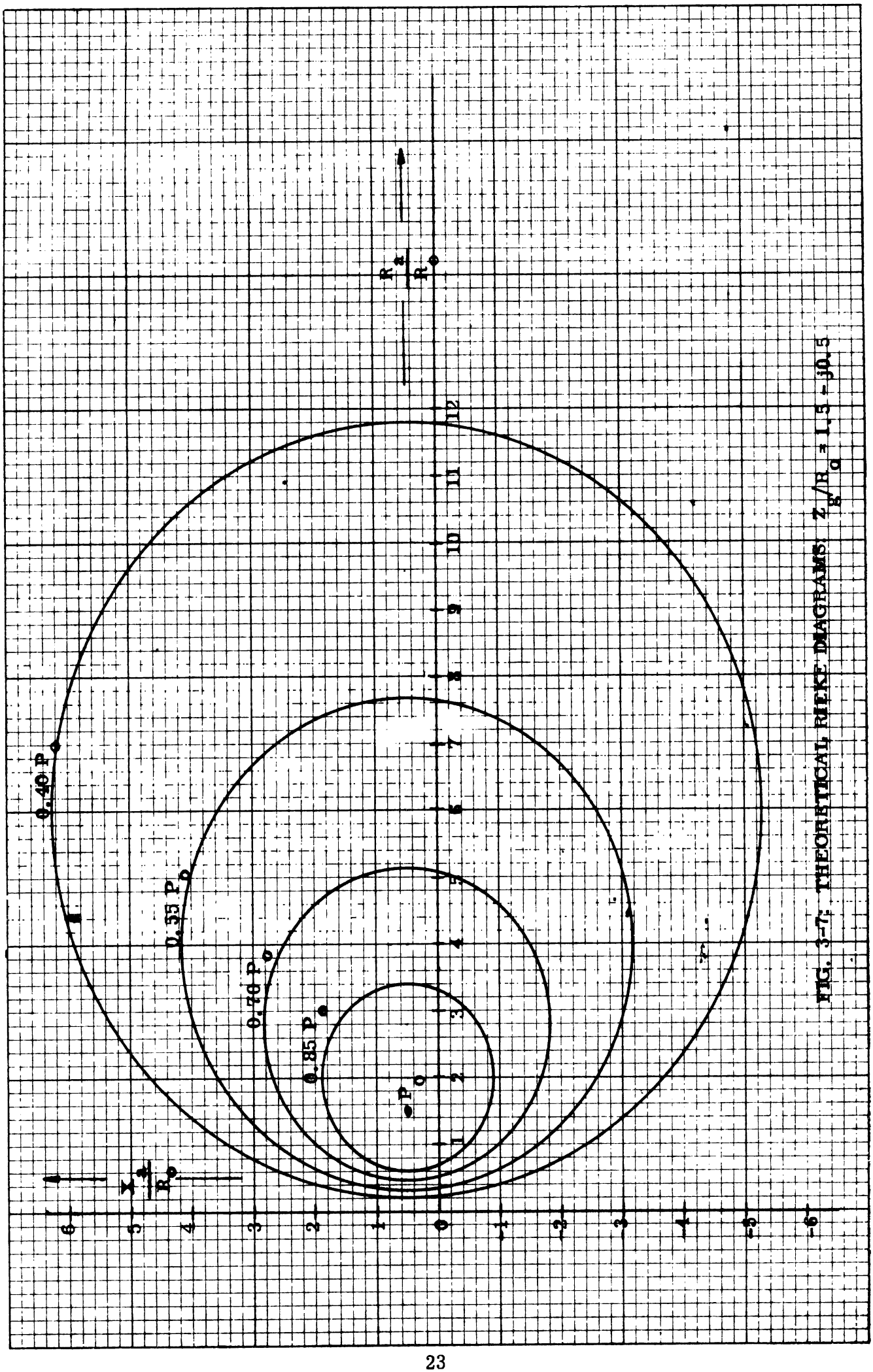

FIG. 3-7: THEORETICAL RIEKE DIAGRAMS: $Z_g/R_a = 1.5 - j0.5$

No GC 19509

DWG NO

DATE

RADIO COMPANY, WEST CONCORD, MASSACHUSETTS

IMPEDANCE OR ADMITTANCE COORDINATES

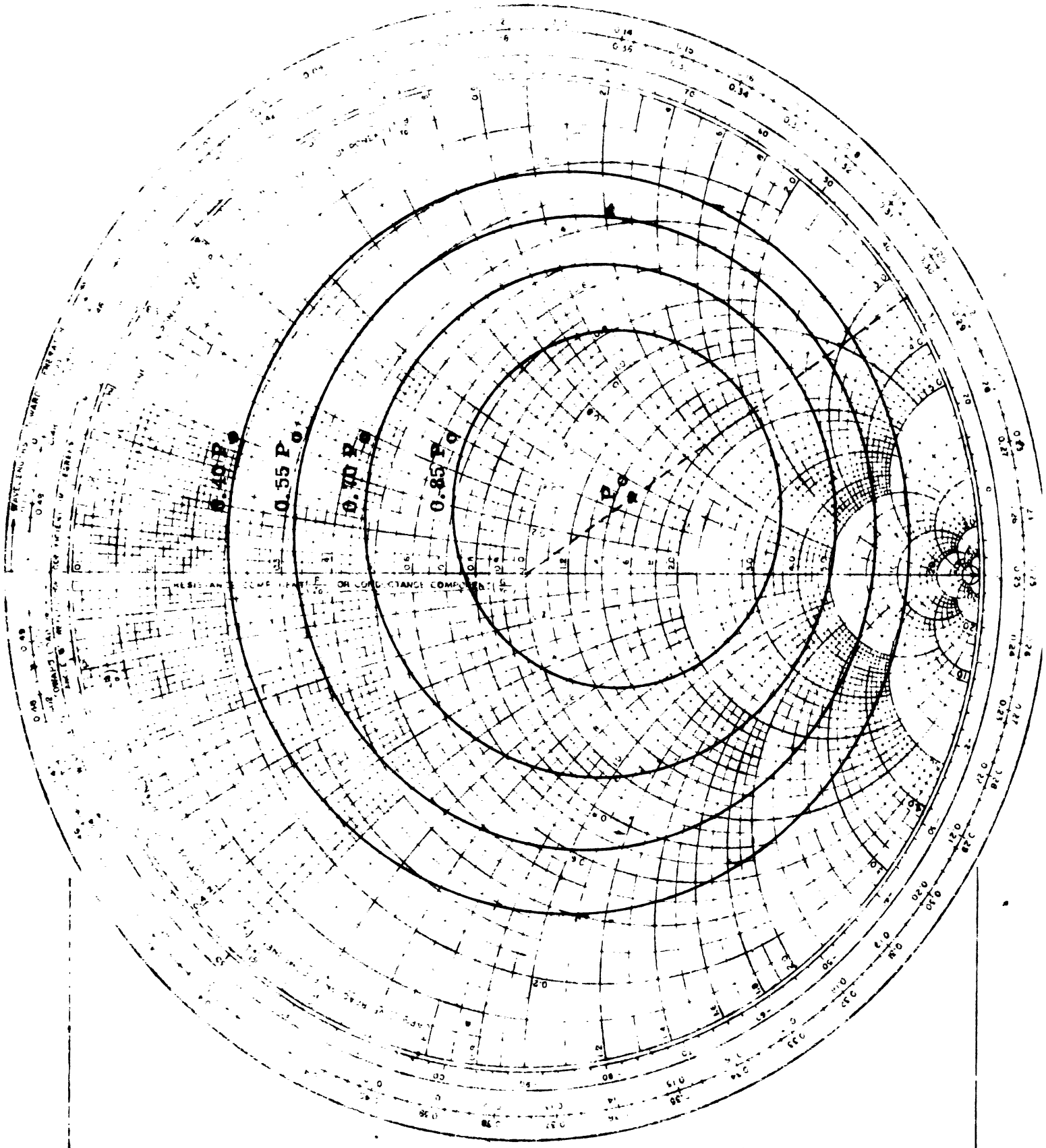

FIG. 3-8: THEORETICAL RIEKE DIAGRAM: $Z/R_o = 1.5 - j0.5$

RADIALLY SCALED PARAMETERS g_o

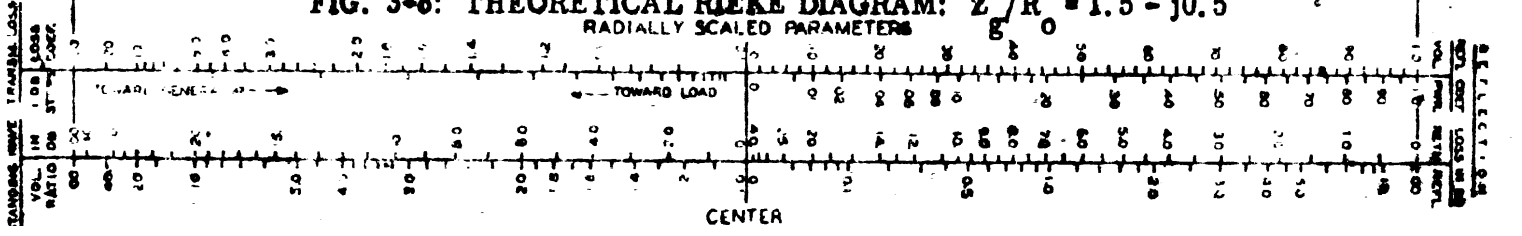

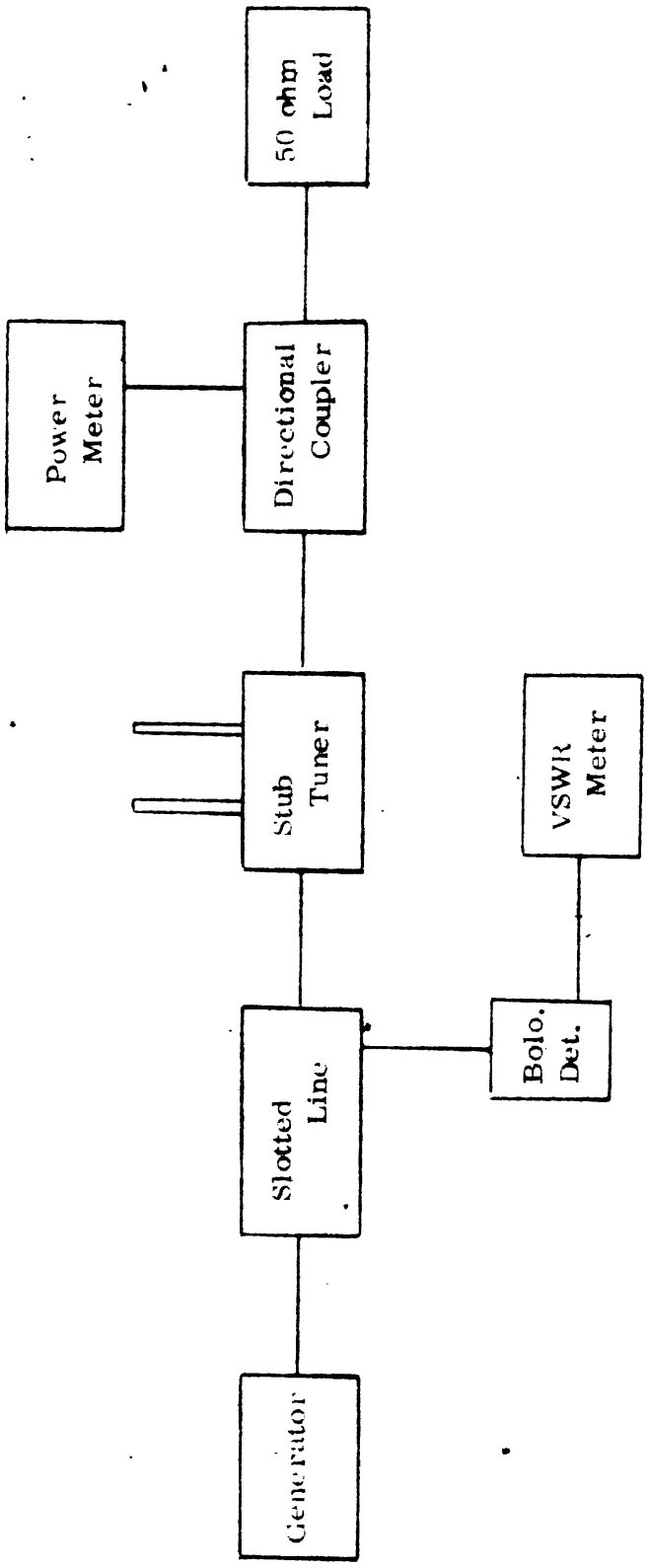

FIG. 3-9: EQUIPMENT BLOCK DIAGRAM FOR EXPERIMENTAL RIEKE DIAGRAMS

NAME		DWG. NO. GC 19509
SMITH-CHASE LABORATORY OF GENERAL RADIO COMPANY, WEST CONCORD, MASSACHUSETTS		DATE

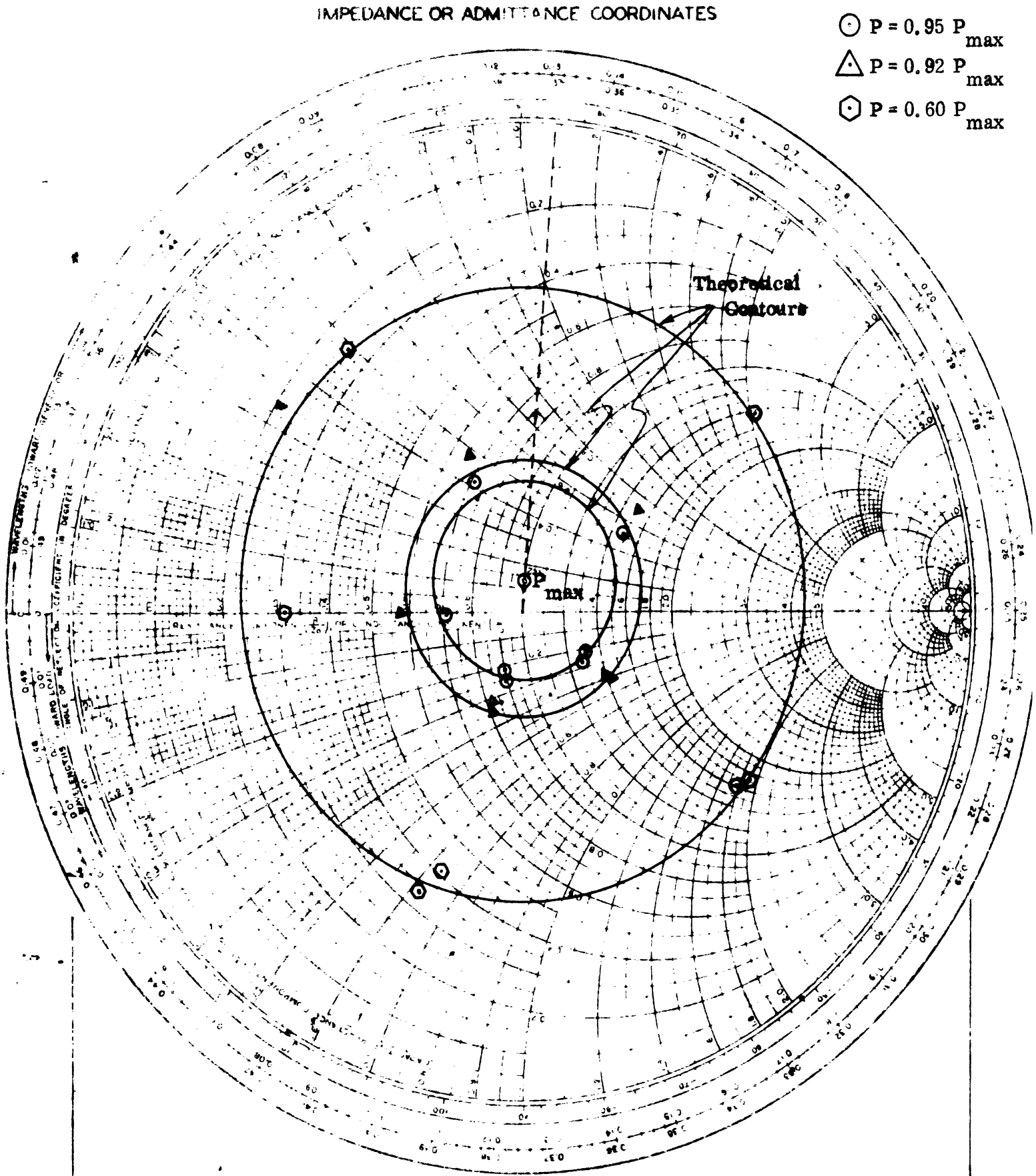

FIG. 3-10: RIEKE DIAGRAM OF H. P. 612-A SIGNAL GENERATOR

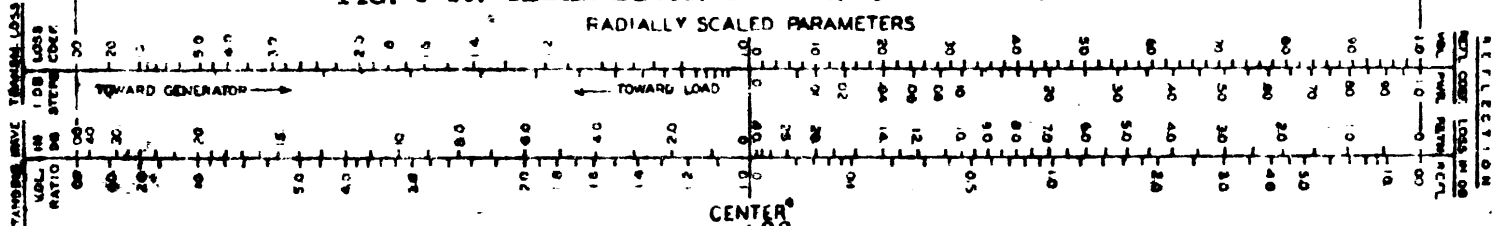

NAME	TITLE	DATE NO.
SMITH CHART From 5301 5560 N	GENERAL RADIO COMPANY, WEST CONCORD, MASSACHUSETTS	SCALE

IMPEDANCE OR ADMITTANCE COORDINATES

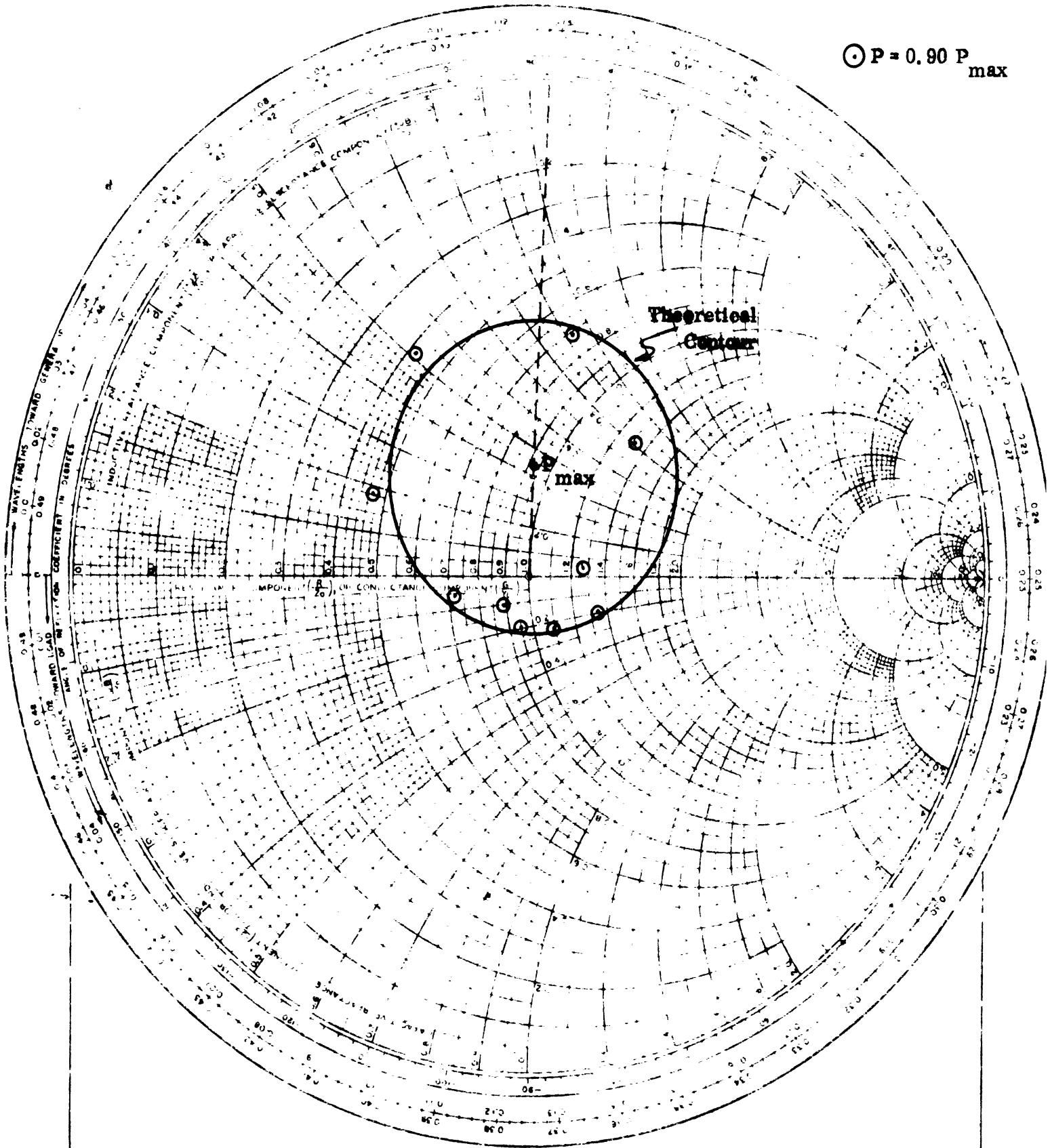

FIG. 3-11: RIEKE DIAGRAM OF TRANSMITTER RT-178/ARC-27

NAME

SMITH CHART FORM 5301 GENERAL RA COMPA MASSA

IMPEDANCE OR ADMITTANCE COORDINATES

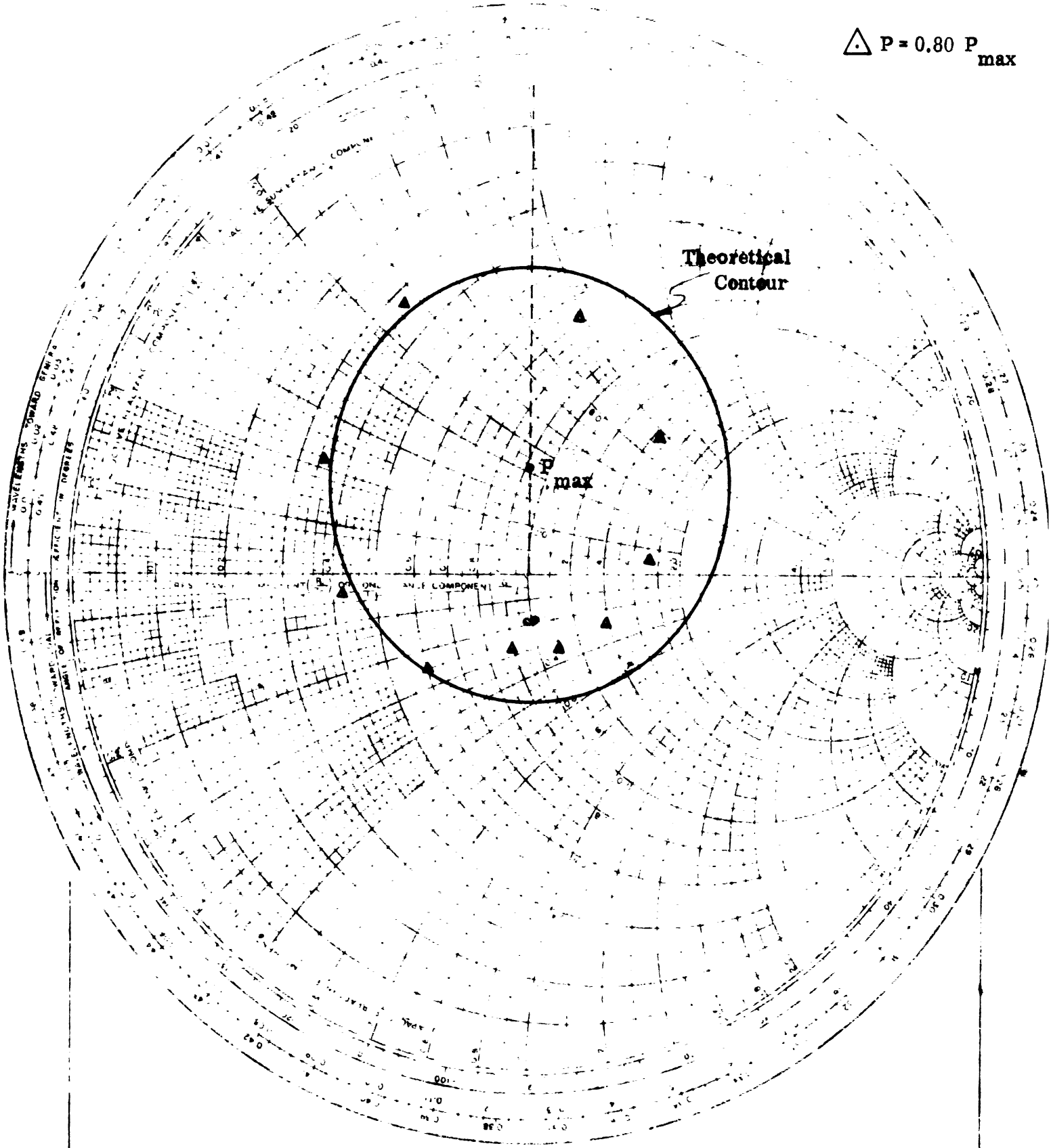

FIG. 3-12: RIEKE DIAGRAM OF TRANSMITTER RT-178/ARC-27

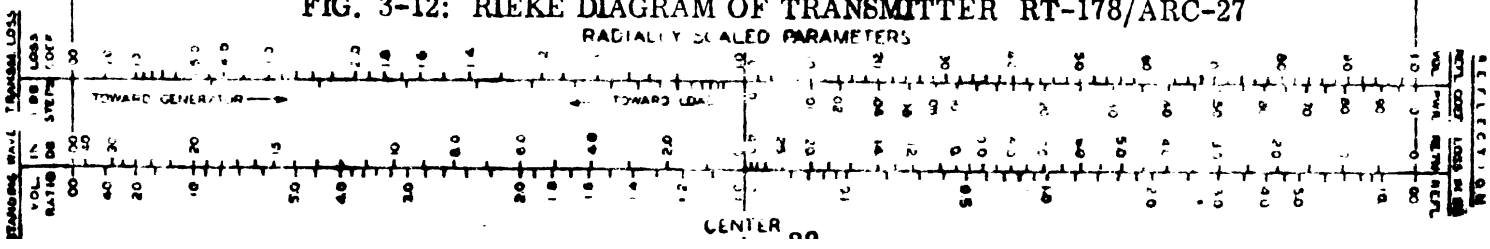

NAME | TITLE | DWG. NO | No.

SMITH CHART FOR Z0 = 75Ω | GENERAL RADIO COMPANY, WEST CONCORD, MASSACHUSETTS | DATE

IMPEDANCE OR ADMITTANCE COORDINATES

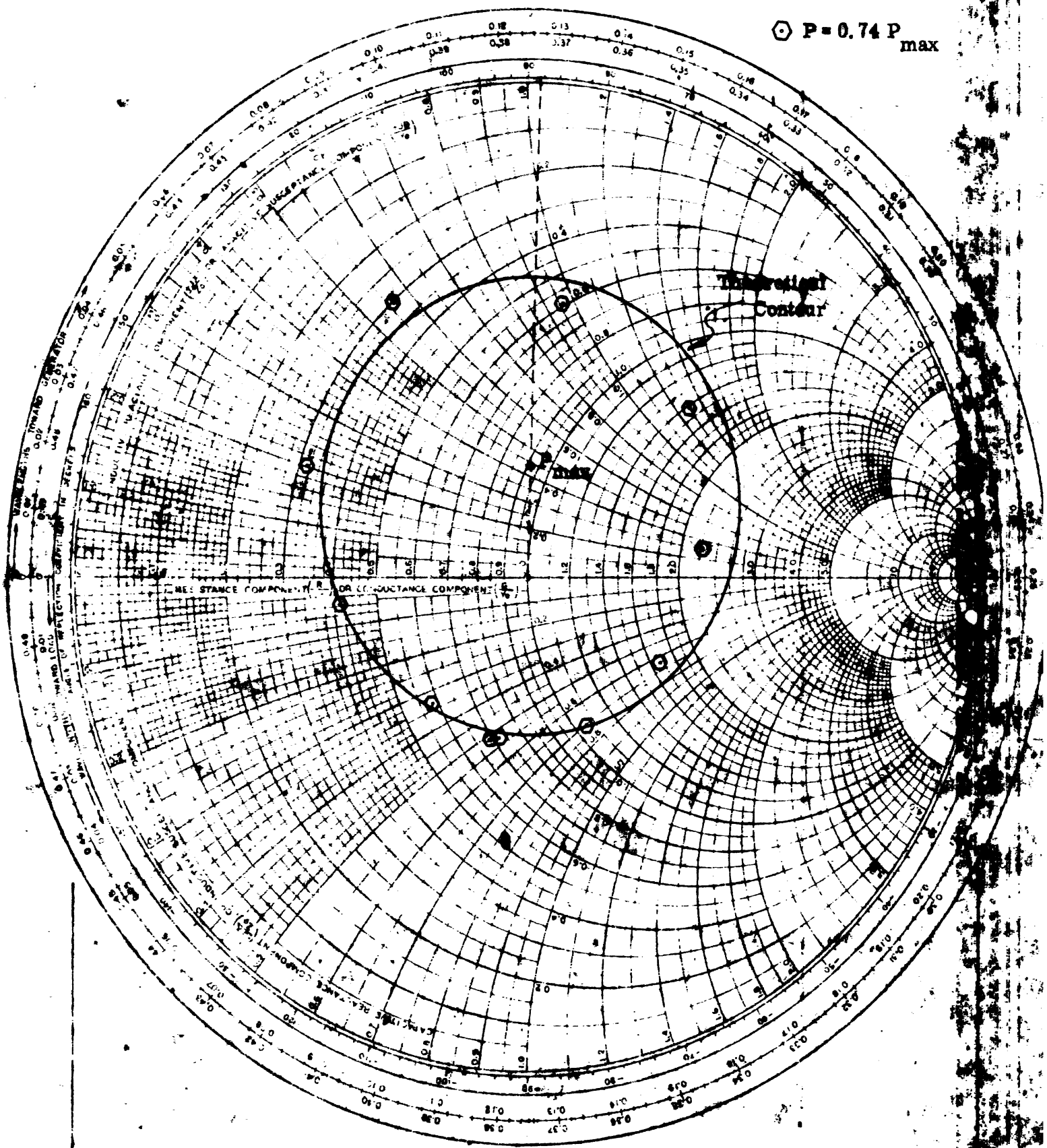

FIG. 3-13: RIEKE DIAGRAM OF TRANSMITTER RT-178/ARC-27

Figure 3-10 is the Rieke diagram of a standard laboratory signal generator. The experimental points conform well with the predicted result. In fact, previous impedance measurements of this generator by another method suggest that the deviations from the theoretical contours are due primarily to experimental error. The signal generator, a Hewlett-Packard 612-A, is of the type shown in the center of Fig. 3-14.

Figures 3-11 to 3-13 are Rieke diagrams of a military type RT-178/ARC-27 transmitter. This experimental data does not conform exactly to the contours drawn from the linear model indicating that the transmitter internal impedance does not remain constant as the load is varied. The transmitter is seen at the right in Fig. 3-14.

Some experimental data was gathered on a third type of source, a laboratory power oscillator. However, a Rieke diagram was not plotted because of the irregular nature of the data obtained. The oscillator, an AIL type 124-A, shown at the left in Fig. 3-14, is of the resonate cavity type. The internal impedance of this oscillator varies drastically with variations of the load impedance.

3.2.3 Conclusions

The method of comparing the Rieke diagrams of a real transmitter and its theoretical linear model provides a graphic, qualitative description of the linearity of the real transmitter. The Rieke diagram of the standard laboratory signal generator exhibits a high degree of linearity. As this result was anticipated, this type of source was chosen to illustrate linear behavior. However, the

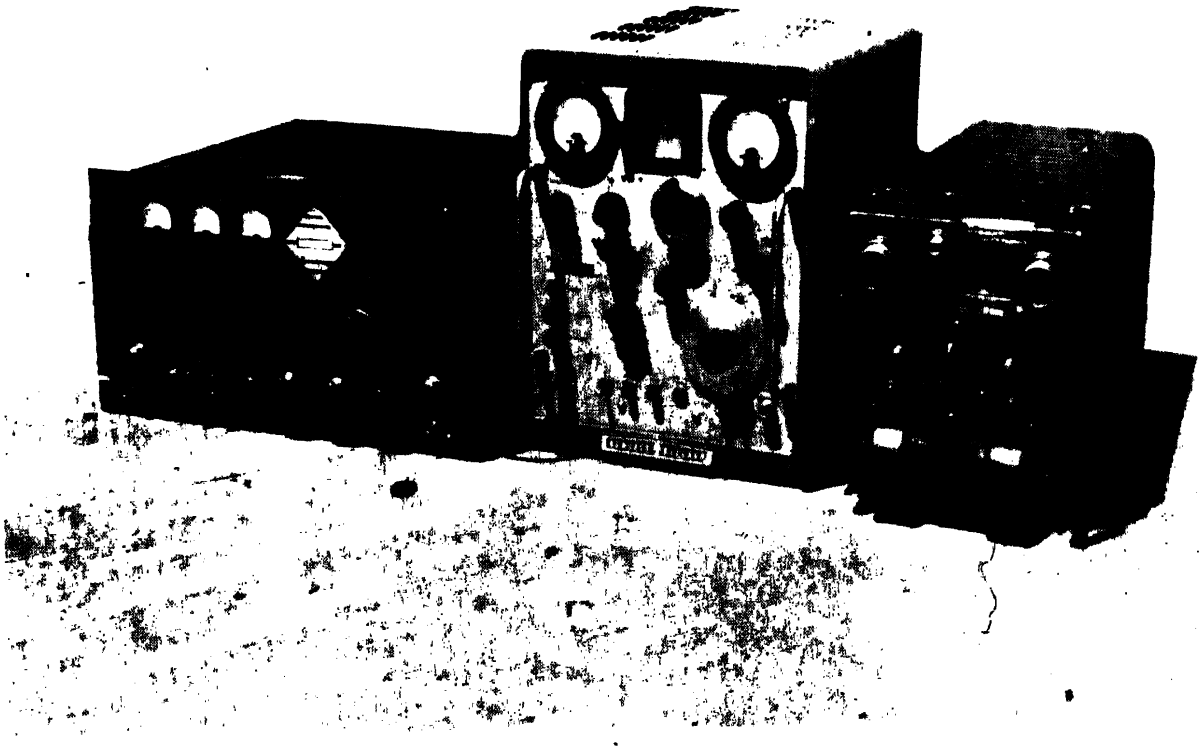

FIG. 3-14: LEFT: AIL POWER OSCILLATOR, TYPE 124-A;
CENTER: STANDARD LABORATORY SIGNAL GENERATOR;
RIGHT: TRANSMITTER RT-178/ARC-27

generator is not of the type used in the field by the military. The AIL power oscillator is of the resonant cavity type and may be found in the field, but experimentation has shown this type of source to be highly non-linear. This oscillator is an example of a source which does not lend itself to measurement of internal impedance by the Michigan developed technique. The Rieke diagrams of the typical service transmitter RT-178/ARC-27 indicate the internal impedance of the transmitter varies slightly with variations of the load impedance, i.e., non-linearity is present, but is relatively small. It is felt that the degree of non-linearity exhibited is not sufficient to cause inaccuracy in the prediction of power transferred to the antenna at the fundamental frequency.

All data presented above is for the fundamental frequency; data for harmonic frequencies has not as yet been collected. It is anticipated that the general character of the data for harmonic frequencies will not differ greatly from that at the fundamental frequency if the transmitter is properly terminated at the fundamental.

Under these conditions, predicition of the power coupled to the antenna promises to be simple and sufficiently accurate. Other variables, such as tuning of the transmitter and variations from transmitter to transmitter of the same type, will need to be investigated to determine their effect on prediction. The variations of source impedance and available power output at each frequency are the important quantities.

3.3 Source Non-Linearity at Harmonic and Spurious Frequencies

Source impedance measurements at harmonic frequencies may be complicated by the non-linearity of the source impedance at the fundamental. Let us denote the source impedance as:

S_1 = source impedance at the fundamental

S_2 = source impedance at the second harmonic

S_n = source impedance at the nth spurious

and the terminating impedance as:

T_1 = terminating impedance at the fundamental

T_2 = terminating impedance at the second harmonic

T_n = terminating impedance at the nth spurious

At present only the variation of S_1 as a function of T_1 has been determined. The variation is present but is relatively small as was seen in Figs. 3-11 to 3-13. Future measurements will involve S_2 versus T_2, S_3 versus T_3 and so on. Inasmuch as the bulk of the transmitter output is dissipated in S_1 and T_1, it is anticipated that the termination T_2, T_3 and so on will not affect S_1 appreciably. In fact, even though no particular attention was paid to the values of T_2, T_3, etc., in the measuring apparatus, no adverse effects were noted.

It is likewise anticipated that if T_1 is maintained at or near the design termination, the impedances S_2, S_3, etc. will be relatively constant with wide variations in T_2, T_3, etc. If this last assumption does not hold, then this approach to the prediction of spurious radiation must be grossly modified or, perhaps, abandoned.

Assume for the purpose of the present discussion that $S_2, \ldots, S_n$ will be relatively constant. It is apparent from measurements made so far that S_1 must be nearly matched to T_1 in order that good measurements can be made. The immediate problem becomes one of providing T_1 to match S_1 while measuring S_2 utilizing a highly reactive load at the second harmonic frequency, and likewise for S_3, S_4, etc.

Some thought has been given to this problem. A cursory examination reveals many ways, using shorted tuning stubs and other apparatus, to produce a nearly pure reactance at any given frequency while maintaining a matched termination at the fundamental frequency. The best method will therefore be that combination of coaxial apparatus which is most conveniently adjusted and calibrated. Work on this problem will proceed as the situation warrants.

REFERENCES

Ferris, J. E. et al (1966), "Investigation of Measurement Techniques For Obtaining Airborne Antenna Spectrum Signatures", Final Report AFAL-TR-66-101, July, 1966, University of Michigan, Radiation Laboratory Report 07274-1-F, 137 pages.

Guillemin, E. A., The Mathematics of Circuit Analysis, pp. 360-373, John Wiley and Sons, Inc., 1949.

Reich, H. J., Philip Ordung, Herbert Krauss, and John G. Skolnik, Microwave Theory and Techniques, D. VanNostrand Co., Inc., Princeton, N. J., 1953, pp. 856-862.